Biosensors and Bioelectronics 132 (2019) 375–381

Contents lists available at ScienceDirect

Biosensors and Bioelectronics

journal homepage: www.elsevier.com/locate/bios

Development of a highly sensitive, quantitative, and rapid detection system for *Plasmodium falciparum*-infected red blood cells using a fluorescent blue-ray optical system

Takeki Yamamoto[a,c], Shouki Yatsushiro[b], Muneaki Hashimoto[b], Kazuaki Kajimoto[b], Yusuke Ido[b], Kaori Abe[b], Yasuyuki Sofue[c], Takahiro Nogami[c], Takuya Hayashi[c], Kenji Nagatomi[c], Noboru Minakawa[d], Hiroaki Oka[c], Toshihiro Mita[a,*], Masatoshi Kataoka[b,**]

[a] Department of Tropical Medicine and Parasitology, Juntendo University School of Medicine, 2-1-1 Hongo, Bunkyo-ku, Tokyo 113-8421, Japan
[b] Health Research Institute, National Institute of Advanced Industrial Science and Technology (AIST), Hayashi-cho 2217-14, Takamatsu 761-0395, Japan
[c] Automotive & Industrial Systems Company, Panasonic Co., 1006 Ooaza-Kadoma, Kadoma, Osaka 571-8506, Japan
[d] Institute of Tropical Medicine, Nagasaki University, 1-12-4 Sakamoto, Nagasaki 852-8523, Japan

ARTICLE INFO

Keywords:
Malaria diagnosis
Compact disc
Highly sensitive detection
Plasmodium falciparum
Fluorescent blue-ray optical system

ABSTRACT

A highly sensitive diagnostic system for determining low-density infections that are missed by conventional methods is necessary to detect the carriers of *Plasmodium falciparum.* A fluorescent blue-ray optical system with a polycarbonate scan disc was developed to detect *P. falciparum*-infected red blood cells (*Pf*-iRBCs), and nine samples could be analyzed simultaneously. The cultured *P. falciparum* strain 3D7 was used to examine the potential of the system for diagnosing malaria. After an RBC suspension had been applied to the disc, the cells were dispersed on the disc by rotation. During the 10 min standing period to allow the RBCs to settle on the disc surface, the cells were simultaneously stained with nuclear fluorescence staining dye Hoechst 34580, which was previously adsorbed on the disc surface. RBCs were arranged on the disc surface as a monolayer by removing excess cells through momentary rotation. Over 1.1 million RBCs remained on the disc for fluorescence analysis. A portable, battery-driven fluorescence image reader was employed to detect fluorescence-positive RBCs for approximately 40 min. A good correlation between examination of Giemsa-stained RBCs by light microscopy and the developed system was demonstrated in the parasitemia range of 0.0001–1.0% by linear regression analysis (R2 = 0.99993). The limit of detection of 0.00020% and good reproducibility for parasitemia determination were observed. The ability of the developed system to detect sub-microscopic low-density *Pf*-iRBCs and provide accurate quantitative evaluation with easy operation was demonstrated.

1. Introduction

Malaria, a mosquito-borne infectious disease, is one of the major human infectious diseases, with an estimated 216 million clinical cases and 445,000 deaths in 2016 (WHO, 2016). Light microscopic examination of red blood cells (RBCs) stained with Giemsa stain is recognized as the gold standard for malaria diagnosis, and it remains widespread as a point-of-care diagnostic procedure in clinical and epidemiological settings (Wu et al., 2015). The procedure for light microscopic examination consists of several steps: collection of finger-prick blood, preparation of thin and thick blood smears, staining with Giemsa stain, and quantitative detection of malaria parasites in the RBCs by microscopic examination. However, this microscopic examination is time consuming, and its accuracy depends on the operator's skill. According to the results of the British laboratories submitted to the Malaria Reference Laboratory, most routine diagnostic laboratories generally achieved a low detection sensitivity [average, 0.01% parasite concentration (parasitemia)] (Milne et al., 1994). Even under optimal conditions for the detection of malaria parasites with excellent blood preparation and skilled technicians, the detection sensitivity is reported to be low (0.001% parasitemia, corresponding to 50 parasites per microliter), and approximately 1 h is required for the examination

* Corresponding author.
** Correspondence to: Biomarker Analysis Group, Health Research Institute, National Institute of Advanced Industrial Science and Technology (AIST), 2217-14 Hayashi-cho, Takamatsu 761-0395, Kagawa, Japan.
E-mail addresses: tmita@juntendo.ac.jp (T. Mita), m-kataoka@aist.go.jp (M. Kataoka).

https://doi.org/10.1016/j.bios.2019.02.064
Received 30 January 2019; Received in revised form 19 February 2019; Accepted 20 February 2019
Available online 07 March 2019
0956-5663/ © 2019 Elsevier B.V. All rights reserved.

(Moody, 2002; Warhurst and Williams, 1996). Antibody-based rapid diagnosis tests (RDT) are often used for malaria diagnosis (Ragavan et al., 2018). Although RDTs have been developed for malaria diagnosis with ease of operation and rapid diagnosis time, the possibility of false-positive and/or false-negative results is a well-known disadvantages of RDTs. The detection sensitivity is similar to that obtained by microscopic examination (McMorrow et al., 2011), and RDTs are not able to quantify malaria parasites in the RBCs. Furthermore, several studies revealed that the sensitivity of HRP2-based RDTs could be compromised due to genetic polymorphism of *Plasmodium. falciparum* HRP2 (Atroosh et al., 2015; Deme et al., 2014; Pava et al., 2010). The sensitivities of light microscopic examination and/or RDT are insufficient for the detection of asymptomatic carriers of *P. falciparum* (Cook et al., 2015; Tiono et al., 2014). Sub-microscopic, low-density malaria infections are considered potential contributors as carriers for ongoing transmission (WHO, 2014, Wu et al., 2015).

High sensitivity of several orders of magnitude greater than those of microscopy and RDTs for the detection of malaria parasites can be achieved by nucleic acid amplification (NAA) techniques such as nested PCR (WHO 2014). However, the disadvantages of NAA tests are that they require a multi-step analysis, are time-consuming and non-quantitative, require costly equipment for analysis and skilled personnel for operation, and lack onsite applicability. Microfabrication techniques are expected to be applied in the field of biomedical analysis (Conde et al., 2016). Peng et al. (2014) reported the use of micromagnetic resonance relaxometry for the rapid and label-free detection of malaria parasites. Recently, a label-free microfluidic cell deformability sensor for the quantitative and high-throughput measurement of malaria parasites has been developed (Yang et al., 2017). However, these devices have not been put into practical use in the field.

In previous studies, we developed a highly sensitive, accurate and quantitative malaria parasite detection system using a cell microarray chip made of polystyrene with 20,944 individually addressable microchambers (Yatsushiro et al., 2010; Yatsushiro et al., 2016). This cell microarray chip was developed to allow the regular dispersion of the RBC suspension with a nucleus-staining fluorescence dye in the microchambers and the formation of a monolayer. The potential of this cell microarray chip system for use in malaria diagnosis was demonstrated by means of monolayer formation of RBCs stained with fluorescence nuclear staining dye and a fluorescence detector equipped with a CCD camera for the detection of fluorescence-positive *P. falciparum*-infected RBCs (*Pf*-iRBCs). Although it only required less than 30 min for analysis per one sample, several steps for handling of this system and power supply for a CCD camera are necessary for malaria diagnosis. For use in a remote area, a diagnostic system with ease of operation and an independent power supply is necessary. Therefore, in the present study, we developed a system with exceptionally higher sensitivity than that of light microscopic examination; the current battery-driven, fluorescenct blue-ray optical system with a scan disc was compact and easy to operate (Fig. 1). After sample application on the scan disc, monolayer formation of RBCs and fluorescent nuclear staining of *Pf*-iRBCs can be performed automatically. Then, *Pf*-iRBCs can be quantitatively detected using an image reader in a short time.

2. Materials and methods

2.1. Construction of the scan disc

The scan disc (EZBNPC01AT, Panasonic Corp. Osaka, Japan; Fig. 1B, D and Fig. 2A i) was constructed from two components, viz., a flow-path disc (Fig. 2A ii) and an optical disc (Fig. 2A iii), and each component was made of polycarbonate by general injection molding. Nine compartmentalized portions were formed by bonding the former with the latter by UV curable adhesion patterned by screen printing method (Lee et al., 2009), thereby allowing nine samples to be analyzed simultaneously on the scan disc. For staining malaria parasites on the scan disc, 180 µl of 0.396 µM Hoechst 34580 (Molecular Probes Inc., Eugene, OR, USA) (Fig. S1), which is a nuclear-specific fluorescence dye (excitation, 392 nm; emission, 440 nm), was injected into each compartmentalized portion of the scan disc and was allowed to be adsorbed at the parasite detection area through lyophilization for storing at room temperature (Fig. 2A iv).

The fluorescent material G3300 (Central Techno Corporation, Osaka, Japan) which emits fluorescence at the excitation wavelength of 400 nm, was mixed in the polycarbonate of the flow path disc. When the scan disc was irradiated with light at 400 nm, which yields strong absorption peak for hemoglobin (Li et al., 2014), RBCs absorbed excitation light, but other portions of the scan disc emitted fluorescence. The presence of G3300 in the flow path disc makes it possible to visualize unstained RBCs on the scan disc. This enabled us to distinguish between the fluorescence spots due to nuclear staining dye in the RBCs as *Pf*-iRBCs and the fluorescence spots outside of RBCs as detection noises, contributing to an improvement in detection accuracy.

2.2. Construction of the fluorescence image reader

The fluorescence image reader (EZBLMOH01T, Panasonic Corp.) was composed of a tablet personal computer (PC) and the main body (Figs. 1C, 2B). The main body included an optical disc drive and field-programmable gate array (FPGA) circuit board. Motions control software (EZBLMO01T-M, Panasonic Corp.) operated the movement of the optical drive and optical pick-up (OPU) via the FPGA board (Figs. 2B.1, 2). After the OPU moved from the standby position to the measuring position, the scan disc set on the image reader was centrifuged by the motor in the disc drive for scanning. The laser in the OPU focused on the surface of the disc and irradiated excitation light. The laser in the OPU emitted light at 405 nm, which is similar to the blue-ray system, as excitation light, and the light was focused on the optical disc through an objective lens, the spot diameter of which was 0.5 µm at the focal point (Fig. 2C). The optical disc had a pitch of the groove and groove to groove length of 0.5 µm, and the optical focal point was positioned along the groove by the conventional focal position adjustment method on the optical disc by the servo method (Bouwhuis et al., 1985). The excitation light scanned the whole detection area to acquire image data at intervals of 0.5 µm from each other. Each image dataset was acquired during each scan of the scan disc. With these specifications, a resolution of 0.5 µm was achieved. Fluorescent signals from the disc and/or fluorescent-stained *Pf*-iRBCs were received by an avalanche photodiode (APD), a light receiving element mounted in the OPU. All acquired image datasets were precisely aligned and a signal two-dimensional image of the whole detection area was constructed by connecting each image dataset (Fig. 2C, D). Alignment of image data was performed on a PC (Fig. 2B.4) via an FPGA circuit board (Fig. 2B.3). With these techniques, it was possible to acquire a high-definition fluorescence image of the whole detection area in a short time as compared with a general fluorescence microscope. The number of RBCs and malaria parasites present in RBCs on the created image were estimated using EZBLMOS01T-A image processing software (Panasonic, Corp.) (Fig. 2B.5).

2.3. Malaria culture

P. falciparum 3D7 cells were cultured in RPMI 1640 medium (Nacalai Tesque, Inc., Tokyo, Japan) supplemented with 50 µg/ml gentamycin (SIGMA-Aldrich Co., St. Louis, MO, USA) and 10% O^+ human serum at a hematocrit of 3%, according to an established method (Trager and Jensen, 1976). Human RBCs (blood group O^+) were obtained from the Japanese Red Cross Society. Parasitemia was calculated by determining the number of *Pf*-iRBCs in 3,000 RBCs and expressed as the ratio to the number of total RBCs. RBCs exhibiting 0.1% parasitemia were added to each plate in 10 ml of culture medium to obtain a final hematocrit of 3%. The plates were then incubated at 37 °C under 5% CO_2, and 90% N_2 gas.

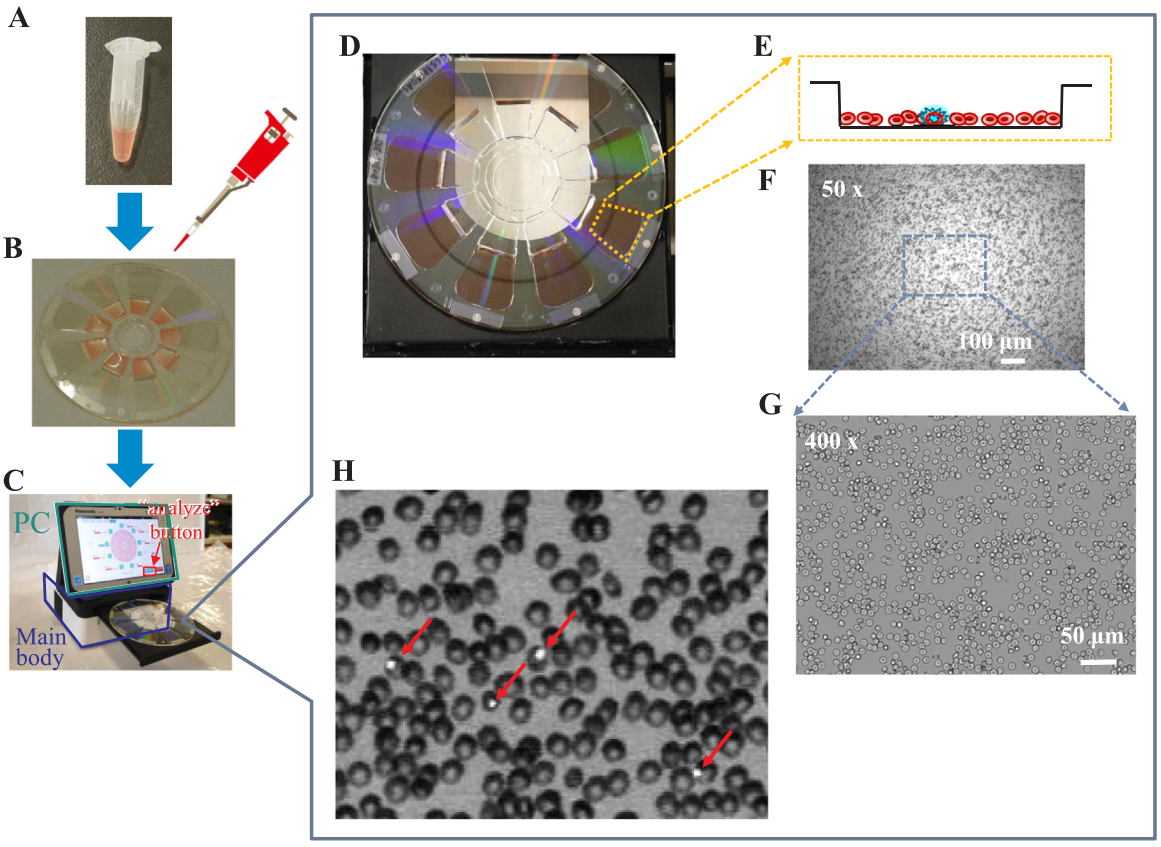

Fig. 1. Schematic depiction of the process for detection of ***Pf***-iRBCs using the fluorescent blue-ray optical system. (A) For analysis on the scan disc, 180-µl samples of *Pf*-iRBCs were prepared. (B) *Pf*-iRBCs were applied to each sample reservoir via a pipette. (C) Picture of the image reader is shown, and the scan disc was placed against the fluorescence image reader. (D) RBCs were analyzed at the detection area. (E) Monolayer formation of RBCs and nuclear fluorescence staining of *Pf*-iRBCs at the detection area. (F, G) Microscopic images of the detection area are shown. (H) Fluorescence image of *Pf*-iRBCs on the disc. The target malaria parasites were analyzed quantitatively at the single-cell level (red arrow, malaria parasite).

For light microscopic examination of *Pf*-iRBCs, 2 µl of malaria culture was smeared to make a thin film on each slide, which was then stained with 5% Giemsa (Merck Co. Ltd., Germany) stain in phosphate-buffered saline (pH 7.2). Thereafter, the slide was examined under a light microscope (Olympus, Co., Ltd., Tokyo, Japan), at a magnification of 1,000× to determine the presence or absence of malaria parasites per 3,000 RBCs (Payne, 1988).

2.4. Detection of Pf-iRBCs on the scan disc

For analyzing cultured *Pf*-iRBCs on the scan disc, an appropriate volume of purified *Pf*-iRBCs suspension was added to PBS to obtain 0.1% and 1.0% parasitemia at a hematocrit of 0.25%. Parasitemia was examined by thin-smear microscopy with Giemsa staining as described previously (Payne, 1988). To obtain 0.0001–0.01% parasitemia samples, serial 10-fold dilution of 0.1% parasitemia samples at a hematocrit of 0.25% with PBS was performed. For analysis on the scan disc, 180 µl of the cultured *Pf*-iRBCs was applied to each sample reservoir (Fig. 1A, B). Then, the scan disc was placed against the fluorescence image reader (Fig. 1C). After the "analyze" button was pushed, the following steps were performed automatically: momentary rotation of the scan disc at 1,000 rpm for 30 s to introduce the *Pf*-iRBC suspension from the sample reservoir into the parasite detection area; 10-min standing to allow RBCs to settle onto the disc surface (Fig. S2), during which time the RBCs were simultaneously stained with Hoechst 34580 that had been previously adsorbed onto the surface of the detection area; removal of excess RBCs by rotation of the disc at 2,000 rpm for 1 min to form a monolayer of RBCs over the entire surface of the detection area; and finally, fluorescence detection of *Pf*-iRBCs at the parasite detection area (Fig. 1D-H). Nine samples on a scan disc could be analyzed simultaneously in approximately 40 min. *Pf*-iRBCs were distinguished from uninfected RBCs based on the fluorescence intensity and size of the fluorescent spot. These fluorescence parameters of individual RBCs were analyzed with the included image processing software. For the discrimination of *Pf*-iRBCs from leukocytes on the scan disc, we employed whole blood from a healthy volunteer to examine the fluorescence intensities and sizes of leukocytes for the analysis.

3. Results and discussion

3.1. Dispersion and monolayer formation of RBCs on the scan disc

The RBC suspension in the sample reservoir of the scan disc was introduced into the detection area through momentary rotation of the disc (Fig. 1D), and the RBCs then settled under gravitational force and adhered to the disc surface as multilayers during 10 min of standing. After rotating the scan disc at 2000 rpm for 1 min, a relatively sparsely formed monolayer of RBCs was observed at the parasite detection area (Fig. 1F, G). The number of dispersed RBCs in the parasite detection area was determined to be 1169623.7 ± 98909 (mean ± standard deviation; n = 67, Fig. S3). Thus, over 1.1 million RBCs per analysis could be examined for the presence of malaria parasites.

3.2. Discrimination between Pf-iRBCs, RBCs, and leukocytes on the scan disc

To identify *Pf*-iRBCs, differential interference-contrast microscopic examination as described previously was employed (Gruring et al.,

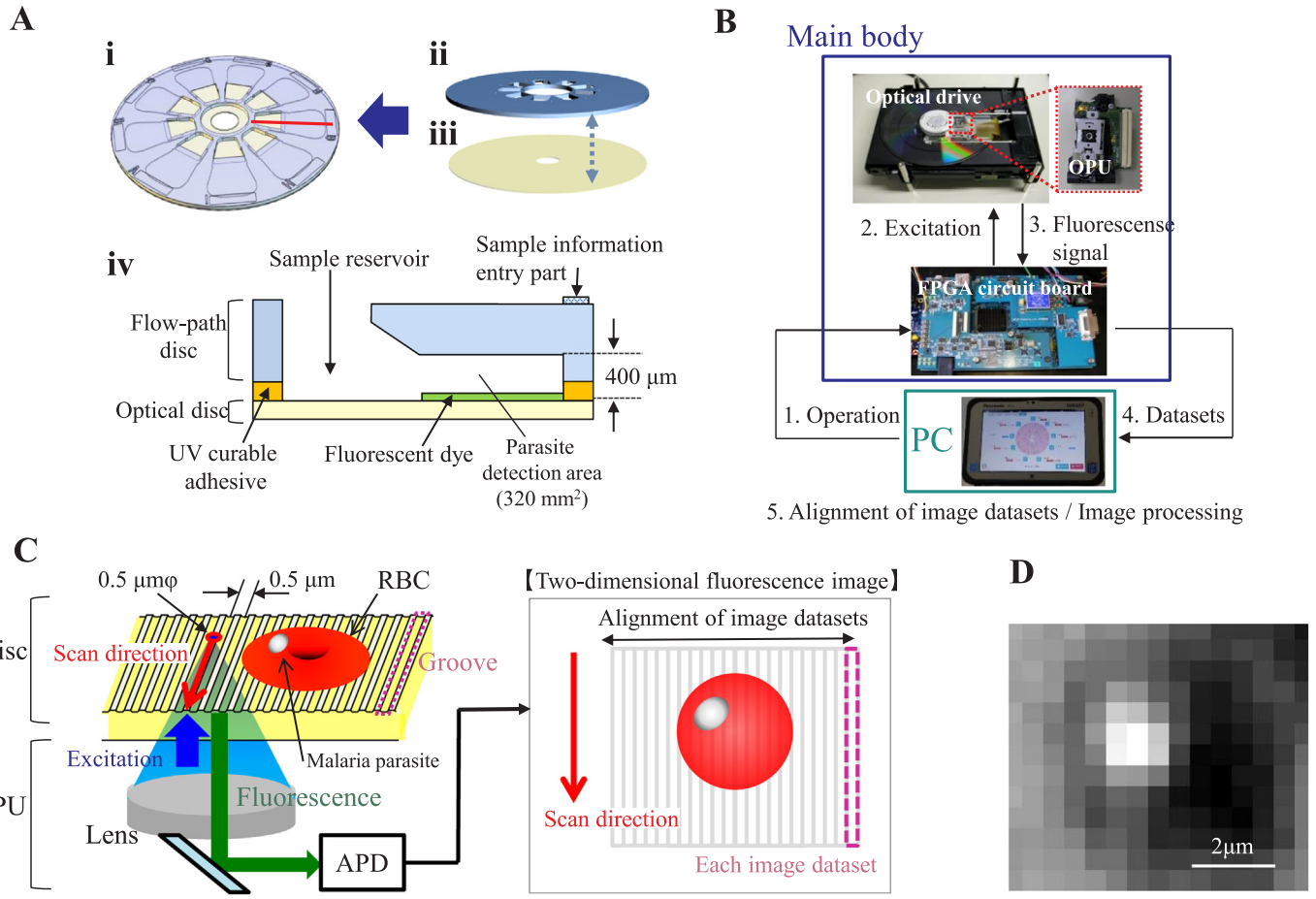

Fig. 2. Construction of the scan disc and the image reader. The scan disc comprises two components, viz., a flow-path disc (A. i) and an optical disc (A. ii), each of which is made of polycarbonate. Nine compartmentalized portions are formed by the bonding of the flow-path disc with the optical disc by the UV-curable adhesion method (A. iii). Schematic diagram of a cross section of the scan disc is shown (A. iv). Image reader internal components and controller (B). Schematic diagram of the optical system using the OPU and acquisition of fluorescence signal from the scan disc, and the processing of two-dimensional images of the acquired fluorescence data are shown (C). Fluorescence image of *Pf*-iRBC on the scan disc (D).

2011). Differential interference-contrast microscopic images of *Pf*-iRBCs (Fig. 3A), leukocytes (Fig. 3B), and non-infected RBCs (Fig. 3C) corresponding to conventional fluorescence microscopic images are shown in Fig. 3 D-F. A fluorescence-positive *Pf*-iRBC was stained with Hoechst 34580 on the scan disc (Fig. 3G and J), and its fluorescence intensity was evidently lower than that of a leukocyte (Fig. 3H, K). The differences in fluorescence intensities must be due to the AT contents in each cell. When we employed Hoechst 34580, a nuclear-specific fluorescence dye that binds to the minor grove of the AT sequence of DNA for the detection of *Pf*-iRBCs on the scan disc, the AT content in the leukocytes was estimated to be approximately 200-times higher than that of *P. falciparum* (Dolezel and Greihuber, 2010; Gardner et al., 2002). As described above, RBCs absorbed 400 nm excitation light due to the presence of hemoglobin, but the other portion (other than areas with RBC adhesion) on the scan disc emitted fluorescence. Uninfected RBCs exhibited very weak fluorescence intensities (Fig. 3I, L). The fluorescence histogram of the entire region of the parasite detection area for each sample was obtained to discriminate RBC adhesion on the scan disc using an image processing software (Fig. S4). The region below the minimal value of the fluorescence intensity was regarded as the RBC region, and the average size of a single RBC which was recognized as an oval silhouette (Fig. 3I), was calculated. Then, the total number of RBCs on the detection area was obtained by the division of the total area of the RBC region by the average size of a single RBC. RBCs that exhibited fluorescence intensities that were 1.4–2.4-times higher than those of uninfected RBCs and had a fluorescent spot with a size from 1.0 μm^2 to 10 μm^2 were considered to be *Pf*-iRBCs (Fig. 3G, J). When the aspect ratio of the fluorescent spot was above 2.4 or its area was below 1.0 μm^2 or above 10 μm^2, this was noted to be detection noise. Therefore, the numbers of RBCs and *Pf*-iRBCs were estimated automatically by using the software to determine parasitemia. The percentage of parasitemia in each sample was determined as follows: number of *Pf*-iRBCs/total number of RBCs × 100.

3.3. Quantification of parasitemia and the examination of selectivity

As shown in Fig. 4A, linear regression analysis of estimated parasitemia obtained by the fluorescent blue-ray optical system and Giemsa microscopy (1.0, 0.1, 0.01, 0.001, and 0.0001%) revealed a significant relationship (R^2 = 0.99993). Data are expressed as the mean ± standard deviation for seven different experiments. An estimate of the parasitemia is of immediate value to the clinician for the determination of the therapeutic strategy and/or prediction of clinical outcome, particularly in the case of *P. falciparum* infection. The limit of detection (LOD) for parasitemia, which yields a signal at 3σ/S [where σ is the standard deviation of blank solutions (n = 32) and S is the slope of the calibration curve (Marella et al., 2018)] was 0.00020% (10 parasites/μl), which was an exceptionally higher sensitivity than that obtained by microscopic examination of blood smears with Giemsa staining. Nested-PCR is often used for the detection of sub-microscopic, low-density malaria infections. The LOD of the developed system was almost compatible with that of nested-PCR (Wang et al., 2014). For malaria

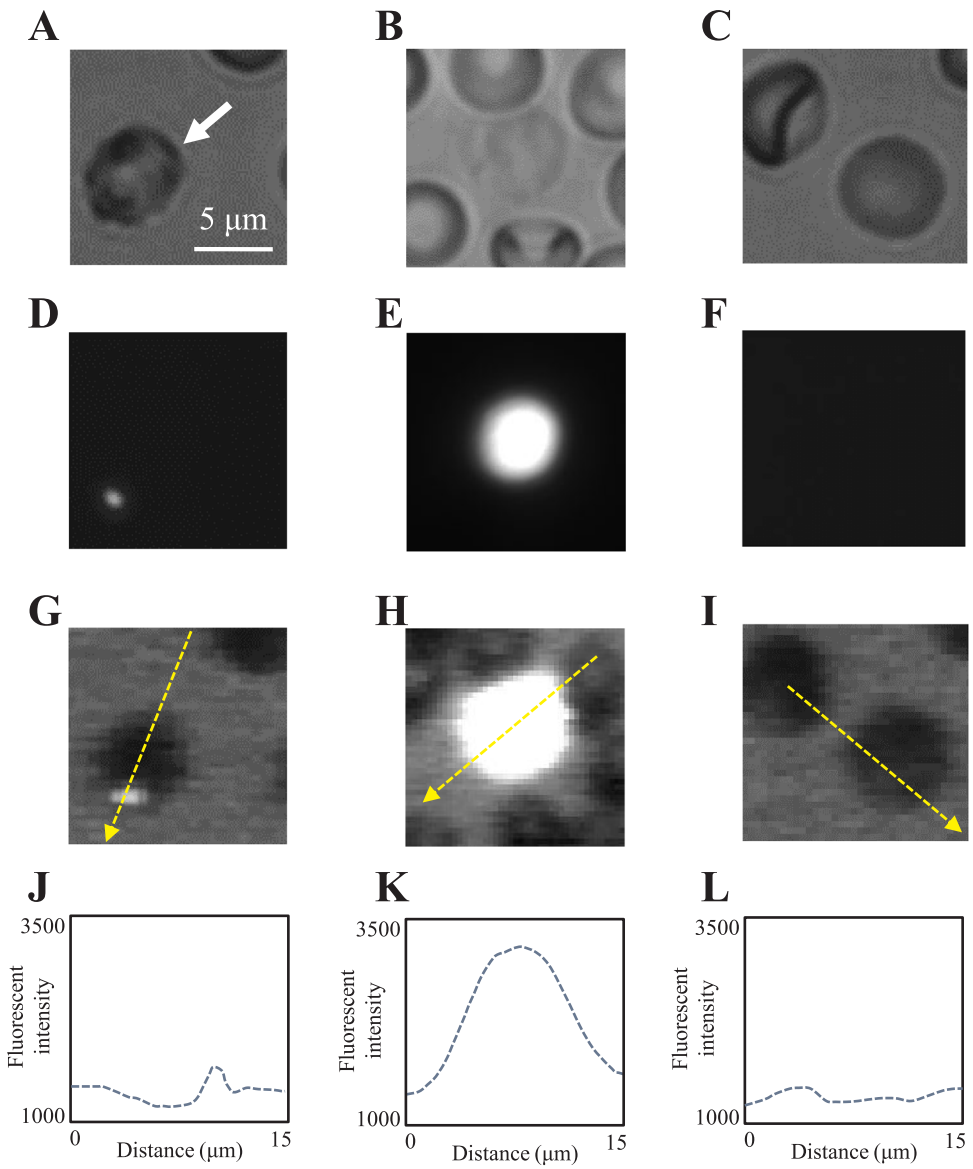

Fig. 3. Discrimination of leukocytes and ***Pf***-iRBCs on the fluorescent blue-ray optical system. Differential interference-contrast microscopic images of *Pf*-iRBCs dispersed on the scan disc. *Pf*-iRBC (A), leukocyte (B), and non-infected RBCs (C) are shown. Conventional fluorescence microscopic images of *Pf*-iRBCs (D), leukocytes (E), and non-infected RBCs (F) are shown. Fluorescence images of *Pf*-iRBCs (G), leukocytes (H), and non-infected RBCs (I) by fluorescent blue-ray image reader. (J-L) Fluorescence- intensity profile along the yellow-dotted arrow in each image is shown (G-I). Fluorescence image of whole RBCs was darker than that of the disc surface through the mixing of the fluorescence material G3300 in the polycarbonate (I, L). Fluorescence intensity of *Pf*-iRBC stained with Hoechst 34580 was apparently higher than that of the disc surface (G, J).

elimination, it is necessary to interrupt transmission, which requires identification and treatment of malaria parasite carriers, both symptomatic and asymptomatic (Britton et al., 2016). Although the minimum number of parasites per microliter of whole blood that perpetuates transmission remains uncertain (Britton et al., 2016), sub-microscopic, low-density malaria infections are considered as potential contributors to ongoing transmission (WHO, 2014; Wu et al., 2015). The current developed fluorescent blue-ray optical system can be employed for the detection of sub-microscopic, low-density infections that are missed by conventional light microscopy and/or RDTs. As shown in Fig. 4B, positive-negative decisions were made on the basis of the critical value (mean + 1.5σ) (Currie, 1968). We found 3 false positive samples in 32 samples of 0% parasitemia and 3 false negative samples in 7 samples of 0.0001% parasitemia. However, there were no false negatives in samples with greater parasitemias (n = 7) than the LOD. Hence, accurate detection of the malaria parasite can be expected at greater parasitemia than the LOD. When the estimated parasitemia in each sample was examined to evaluate the reproducibility of quantification of parasitemia in the different parasite detection areas (Fig. 4C), we could observe good reproducibility in a parasitemia-dependent manner. This phenomenon may be due to the relatively low effect of the presence of the background on the detection of fluorescence-positive RBCs in high-parasitemia samples compared with that of low-parasitemia sample.

Our developed system is portable, easy to operate, and battery-driven for 6 h which is suitable for field use (Table 1). Although the stability of lyophilized Hoechst 34580 on the scan disc has not been confirmed, we have already confirmed several months of stability at room temperature of another nuclear staining dye for the detection of *P. falciparum*, SYTO 41, which is more unstable than Hoechst 34580 (data not shown). Thus, the satisfactory stability of Hoechst 34580 on the disc for field use can be expected. The removal of leukocytes from whole blood is necessary prior to application of samples on the scan disc. This requires an electricity supply and some apparatus for the conventional centrifugation to remove leukocytes, and this is not suitable for field use. In a previous study, we developed a push column with silicon oxide (SiO_2) nano-fibers without any power supply to separate leukocytes from whole blood (Yatsushiro et al., 2016). We will, thus, employ this push column with SiO_2 nano-fibers in a future prospective experimental study utilizing our current fluorescent blue-ray optical system for malaria diagnosis in the field.

4. Conclusion

In this study, we developed a potential nuclear fluorescent staining

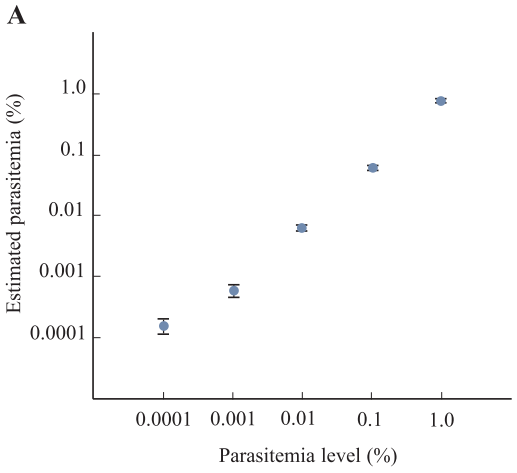

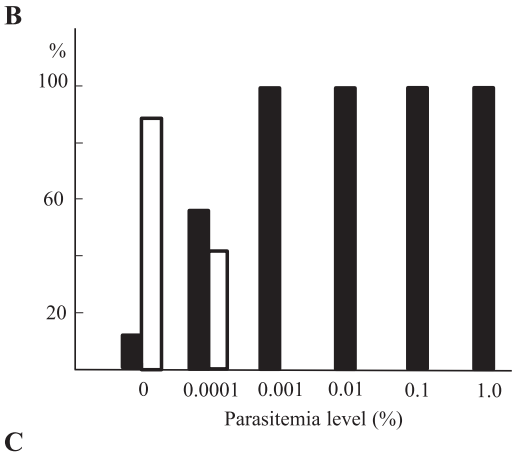

C

Parasitemia detection area	Parasitemia (%)				
	0.0001	0.001	0.01	0.1	1.0
1	0.000160	0.000828	0.00654	0.0869	0.845
2	0.000162	0.000478	0.00612	0.0815	0.931
3	0.000170	0.000431	0.00690	0.0778	0.850
4	0.000175	0.000577	0.00791	0.0875	0.911
5	0.000175	0.000790	0.00715	0.0833	0.886
6	0.000237	0.000517	0.00587	0.0776	0.842
7	0.000087	0.000519	0.00694	0.0760	0.856
Average	0.000167	0.000591	0.00678	0.0815	0.874
RSD (%)	26.40	26.28	10.06	5.68	4.05

RSD, relative standard deviation.

Fig. 4. Comparative analysis of the estimated parasitemia obtained with the fluorescent blue-ray optical system and conventional Giemsa staining microscopic method. Linear regression analysis was used. The number of fluorescence-positive RBCs was determined for each parasitemia samples. Data are expressed as the mean ± standard deviation for seven different experiments (A). The frequencies of false positive and false negative at 0.0001%, 0.001%, 0.01%, 0.1%, and 1.0% parasitemia are shown (B). Solid bars show positive and open bars showed negative results.
Reproducibility for parasitemia determination in the different parasite detection area was examined (C).

Table 1
Comparison of properties of practical methods for malaria diagnosis in field use.

	Giemsa stained microscopy	Rapid diagnosis test	Method in our study
Limit of detection Parasites/μl	50–500	100–200[a]	10
Quantitativity	Yes	No	Yes
Difficulty in diagnosis	Difficult[b]	Easy	Easy
Time required for diagnosis	60 min	15~20 min	40 min/9 samples
Cost	Very inexpensive	$0.6~1.2[c]	$1.0/test[d]

[a] Referred from McMorrow et al. (2011)
[b] Accuracy is exacting and depends on a good staining and well-supervised technicians
[c] Referred from Jimenez et al. (2017)
[d] Target price

method for exceptionally highly sensitive and quantitative detection of *Pf*-iRBCs in the RBC monolayer formed on the scan disc. Automatic fluorescence analysis can be performed after applying and enclosing the sample on the scan disc to prevent exposure of the blood samples to the end user. Our developed system will be applicable for field use.

CRediT authorship contribution statement

Takeki Yamamoto: Conceptualization, Data curation, Formal analysis, Investigation, Methodology, Software, Visualization, Writing - original draft, Writing - review & editing. **Shouki Yatsushiro:** Conceptualization, Investigation. **Muneaki Hashimoto:** Conceptualization, Data curation, Formal analysis, Investigation, Methodology. **Kazuaki Kajimoto:** Investigation. **Yusuke Ido:** Investigation. **Kaori Abe:** Investigation. **Yasuyuki Sofue:** Investigation, Methodology. **Takahiro Nogami:** Investigation, Methodology. **Takuya Hayashi:** Investigation, Methodology. **Kenji Nagatomi:** Investigation, Methodology. **Noboru Minakawa:** Conceptualization, Resources, Validation. **Hiroaki Oka:** Conceptualization, Data curation, Funding acquisition, Methodology, Project administration, Resources, Software, Validation. **Toshihiro Mita:** Conceptualization, Data curation, Funding acquisition, Validation. **Masatoshi Kataoka:** Conceptualization, Data curation, Formal analysis, Funding acquisition, Methodology, Project administration, Resources, Supervision, Validation, Visualization, Writing - original draft, Writing - review & editing.

Acknowledgement

This research was supported by AMED (Japan Agency for Medical Research and Development) under Grant Number JP15km0908001 and by the GHIT (Global Health Innovative Technology Fund) (G2015-210). Approvement of this study was obtained from institutional review board in Juntendo University (2014168).

Conflict of interest

The authors declare no conflict of interest.

Author contributions

T. K., S, Y., M. H., N. M., H. O., T. M., and M. K. conceived and designed the experiments. T. K., S. Y., M. H., K. K., Y. I., K. A., Y. S., T. N., T. H., and K. N. performed the experiments. T. K., M. H., Y. S., T. N., T. H., K. N., H. O., T. M., and M. K. analyzed the data. T. K., S. Y., M. N, K. K., Y. I., K. A., Y. S., T. N., T. H., and K. N. contributed reagents /materials/analysis tools. T. K., and M. K. wrote the manuscript. All authors reviewed the manuscript.

Declaration of interest statement

To the best of our knowledge, the named authors have no conflict of interest, financial or otherwise

Appendix A. Supporting information

Supplementary data associated with this article can be found in the online version at doi:10.1016/j.bios.2019.02.064.

References

Atroosh, W.M., Al-Mekhlafi, H.M., Al-Jasari, A., Sady, H., Al-Delaimy, A.K., Nasr, N.A., Dawaki, S., Abdulsalam, A.M., Ithoi, I., Lau, Y.L., Fong, M.Y., Surin, J., 2015. Parasit. Vectors 8, 388.
Bouwhuis, G., Braat, J., Huijser, A., Pasman, J., van Rosmalen, G., Schouhamer, I.K., 1985. Principles of Optical Disc Systems. Adam Hilger Ltd, Bristol.
Britton, S., Cheng, Q., McCarthy, J.S., 2016. Malar. J. 15, 88.
Conde, J.P., Madaboosi, N., Soares, R.R., Fernandes, J.T., Novo, P., Moulas, G., Chu, V., 2016. Essays Biochem. 60, 121–131.
Cook, J., Xu, W., Msellem, M., Vonk, M., Bergstrom, B., Gosling, R., Al-Mafazy, A.W., McElroy, P., Molteni, F., Abass, A.K., Garimo, I., Ramsan, M., Ali, A., Martensson, A., Bjorkman, A., 2015. J. Infect. Dis. 211, 1476–1483.
Currie, L.A., 1968. Anal. Chem. 40, 586–593.
Dolezel, J., Greihuber, J., 2010. Cytometry A 77 (635), 642.
Deme, A.B., Park, D.J., Bei, A.K., Sarr, O., Badiane, A.S., Gueye, Pel, H., Ahouidi, A., Ndir, O., Mboup, S., Wirth, D.F., Ndiaye, D., Volkman, S.K., 2014. Malar. J. 13, 34.
Gruring, C., Heiber, A., Kruse, F., Ungefehr, J., Gilberger, T.W., Spiemann, T., 2011. Nat. Commun. 2, 165.
Jimenez, A., Rees-Channer, R.R., Perera, R., Gamboa, D., Chiodini, P.L., González, I.J., Mayor, A., Ding, X.C., 2017. Malar J. 16, 128.
Lee, B.S., Lee, J.N., Park, J.M., Lee, J.G., Kim, S., Cho, Y.K., Ko, C., 2009. Lab Chip 9, 1548–1555.
Li, P., Zhao, Z., Wang, Y., Xing, H., Parker, D.M., Yang, Z., Baum, E., Li, W., Sattabongkot, J., Sirichaisinthop, J., Li, S., Yan, G., Cui, L., Fan, Q., 2014. Malar. J. 13, 175.
Marella, V., Lalitha, K., Pravallika, M., Nalluri, B.N., 2018. Pharm. Methods 9, 45–48.
McMorrow, M.L., Aidoo, M., Kachur, S.P., 2011. Clin. Microbiol. Infect. 17, 1624–1631.
Milne, L.M., Kyi, M.S., Chiodini, P.L., Warhurst, D.C., 1994. J. Clin. Pathol. 47, 740–742.
Moody, A., 2002. Clin. Microbiol. Rev. 15, 66–78.
Pava, Z., Echeverry, D.F., Diaz, G., Murillo, C., 2010. Am. J. Trop. Med. Hyg. 83, 834–837.
Payne, D., 1988. Bull. World Health Organ. 66, 621–626.
Peng, W.K., Kong, T.F., Ng, C.S., Chen, L., Huang, Y., Bhagat, A.A., Nguyen, N.T., Preiser, P.R., Han, J., 2014. Nat. Med. 20, 1069–1073.
Ragavan, K.V., Kumar, S., Swaraj, S., Neethirajan, S., 2018. Biosens. Bioelectron. 105, 188–210.
Tiono, A.B., Ouedraogo, A., Diarra, A., Coulibaly, S., Soulama, I., Konate, A.T., Barry, A., Mukhopadhyay, A., Sirima, S.B., Hamed, K., 2014. Malar. J. 13, 30.
Trager, W., Jensen, J.B., 1976. Science 193, 673–675.
Wang, B., Han, S.S., Cho, C., Han, J.H., Cheng, Y., Lee, S.K., Galappaththy, G.N., Thimasarn, K., Soe, M.T., Oo, H.W., Kyaw, M.P., Han, E.T., 2014. J. Clin. Microbiol. 52, 1838–1845.
Warhurst, D.C., Williams, J.E., 1996. J. Clin. Pathol. 49, 533–538.
WHO, 2014. Global Malaria Program. WHO, Switzerland.
WHO, 2016. World Malaria Report 2017. WHO, Switzerland (World Malaria Report).
Wu, L., van den Hoogen, L.L., Slater, H., Walker, P.G., Ghani, A.C., Drakeley, C.J., Okell, L.C., 2015. Nature 528, S86–S93.
Yang, X., Chen, Z., Miao, J., Cui, L., Guan, W., 2017. Biosens. Bioelectron. 98, 408–414.
Yatsushiro, S., Yamamoto, T., Yamamura, S., Abe, K., Obana, E., Nogami, T., Hayashi, T., Sesei, T., Oka, H., Okello-Onen, J., Odongo-Aginya, E.I., Alai, M.A., Olia, A., Anywar, D., Sakurai, M., Palacpac, N.M., Mita, T., Horii, T., Baba, Y., Kataoka, M., 2016. Sci. Rep. 6, 30136.
Yatsushiro, S., Yamamura, S., Yamaguchi, Y., Shinohara, Y., Tamiya, E., Horii, T., Baba, Y., Kataoka, M., 2010. PLoS One 5, e13179.